

Pressure shift of the zone-center TO mode of Zn

H. Olijnyk and A. P. Jephcoat

Department of Earth Sciences, University of Oxford, Oxford OX1 3PR, United Kingdom

D. L. Novikov

Arthur D. Little Inc., Acorn Park, Cambridge, Massachusetts 02140-2390

N. E. Christensen

Institute of Physics and Astronomy, University of Aarhus, DK-8000 Aarhus C, Denmark

(Received 11 February 2000)

The pressure dependence of the transverse-optical zone-center phonon mode of Zn was measured by means of Raman spectroscopy up to 58 GPa at room temperature. The frequency increases under pressure and no anomaly is observed in the pressure range around 10 GPa where electronic topological transitions are expected to occur, and where also *ab initio* “frozen phonon” calculations predict a weak anomaly in the c/a ratio. The relatively large value of the mode Grüneisen parameter $\gamma_i = -d \ln \nu_i / d \ln V$ and its strong decrease under pressure are related to the high compressional anisotropy at ambient pressure and the gradual anisotropic \rightarrow isotropic transition occurring with increasing pressure in Zn, respectively. An irregularity is observed in the pressure dependence of the line width around 10 GPa which may be related to changes in the phonon-phonon and electron-phonon interactions that could be a consequence of the electronic topological transitions.

I. INTRODUCTION

At ambient conditions Zn crystallizes in the hexagonal close-packed (hcp) structure with an exceptionally large c/a axial ratio of 1.856, compared to 1.633 for the ideal hcp structure. Under compression the c/a ratio decreases continuously^{1–7} and in some x-ray-diffraction studies^{1,5,6} an anomaly associated with a change in slope of c/a with pressure was observed around 9–10 GPa corresponding to a relative volume $V/V_0 = 0.886$ according to Ref. 6.

Various first-principles calculations applying different approximations find an anomaly in the c/a ratio at reduced volume with values ranging from $V/V_0 \approx 0.88$ –0.92 and also suggest the occurrence of one or more electronic topological transitions (ETT) in this compression range which apparently lead to the crystallographic anomalies.^{8–11} High-pressure Mössbauer studies reported a sharp drop of the Lamb-Mössbauer factor f at 6.6 GPa and 4 K in Zn indicating a drastic decrease of low-frequency acoustic and optical phonons, also interpreted as a result of an ETT.^{12,13} Inelastic neutron-scattering experiments by Morgan *et al.*¹⁴ at room temperature to 8.8 GPa of the transverse acoustic branch Σ_3 showed a very rapid increase of the mode Grüneisen parameter γ_i above 6.8 GPa which was attributed to a giant Kohn anomaly. Morgan *et al.*¹⁴ argued that phonon softening may occur at pressures higher than 8.8 GPa through collapse of the Kohn anomaly via an ETT. Subsequent inelastic n -scattering studies to 9.4 GPa by Klotz *et al.*¹⁵ of acoustic phonon modes found regular behavior of the Σ_3 , Σ_4 , and T_4 modes, i.e., the anomaly found by Morgan *et al.*¹⁴ could not be verified, and their lattice-dynamical calculations demonstrated that the strong decrease in f cannot be due to $k=0$ phonon modes sensitive to the occurrence of an ETT.

The most recent x-ray-diffraction study,⁷ however, reveals that there is no anomaly in the volume dependence of the c/a

ratio in Zn at room temperature and associates the previous findings with nonhydrostatic effects. In this context it should be noted that there were arguments¹⁵ that the change of f might be an artifact due to a phase transition in the pressure transmitting medium used in the Mössbauer experiments.

In the present paper we report on high-pressure studies of the zone-center TO mode of Zn by high precision Raman spectroscopy. These data are compared with first-principles calculations of the pressure shift of this phonon mode. Although the theory finds ETT's for pressures near 10 GPa, no frequency anomaly is found when numerical scatter is taken into account.

II. EXPERIMENT

Polycrystalline Zn samples with an approximate thickness of 10 μm were loaded into the gasket hole of a high-pressure diamond-anvil cell. In one run helium, loaded at 0.2 GPa,¹⁶ was used as a pressure-transmitting medium to ensure the best possible hydrostatic conditions, while a further run was performed with 4:1 methanol:ethanol as a pressure transmitting medium, which is hydrostatic only below 10 GPa. Pressures were determined by the ruby fluorescence method.^{17,18} Raman spectra were obtained at room temperature with the 514.5-nm (mainly) and the 488-nm lines of an Ar⁺ laser. Scattered light was analyzed at an angle of 135° with respect to the exciting laser beam using a 0.6-m triple spectrograph and a liquid-nitrogen-cooled, charge-coupled device, multichannel detector. Before and after each Raman measurement calibration spectra of a Ne lamp were recorded to correct for small drifts in the energy calibration of the spectrometer due to changes in laboratory temperature. Laser power was held low enough to avoid heating of the sample. The peak positions were determined by fitting Voigt-profiles to the Raman peaks. These procedures ensured a relative

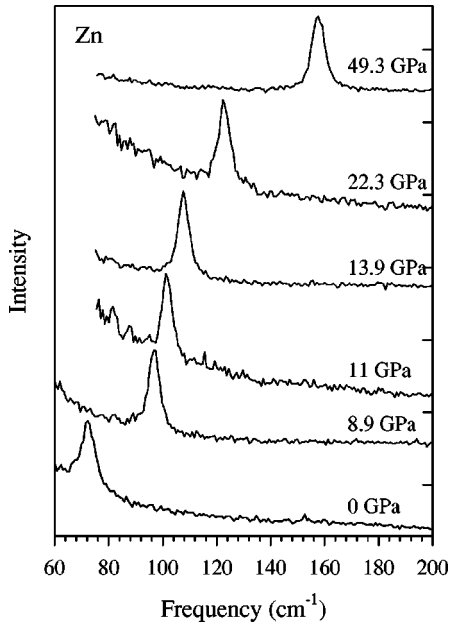


FIG. 1. Raman spectra of the E_{2g} mode of Zn at various pressures with He as pressure-transmitting medium.

precision in the determination of the Raman frequencies within 0.2 cm^{-1} , necessary to resolve slight frequency discontinuities.

III. THEORY

The theoretical phonon frequencies are obtained from density-functional calculations of the shifts in total energy caused by small displacements of the atomic coordinates in a pattern defined by the mode considered. The energy term of second order in the displacement then yields the phonon frequency. This method is the so-called “frozen-phonon” calculation (lowest Born-Oppenheimer approximation). Only the E_{2g} mode is of interest for comparison to Raman data, but we calculated nevertheless also the pressure variation of B_{1g} , and these results will also be included.

The one-electron equations were solved by means of the linear muffin-tin orbital (LMTO) method,¹⁹ and we apply a full-potential implementation.^{20,21} We did not apply the straight local-density approximation (LDA), but have chosen rather to use a generalized-gradient approximation (GGA), in this case the version suggested by Perdew, Burke, and Ernzerhof.²² The reason for this is, as discussed in Refs. 10 and 11, that the LDA leads to a very strong overbinding in the case of Zn. The equilibrium volume obtained by LDA calculations is 11% too small. The GGA, on the other hand, leads to a pressure-volume relation which agrees very well with experiments. (But, as discussed earlier,²³ there are other ways in which equally good results can be obtained.)

The theoretical pressure P was obtained from calculations of the total energy E as a function of volume V . At each volume the axial ratio c/a was varied as to minimize the energy. The detailed variation of a and c with pressure is described in Ref. 10.

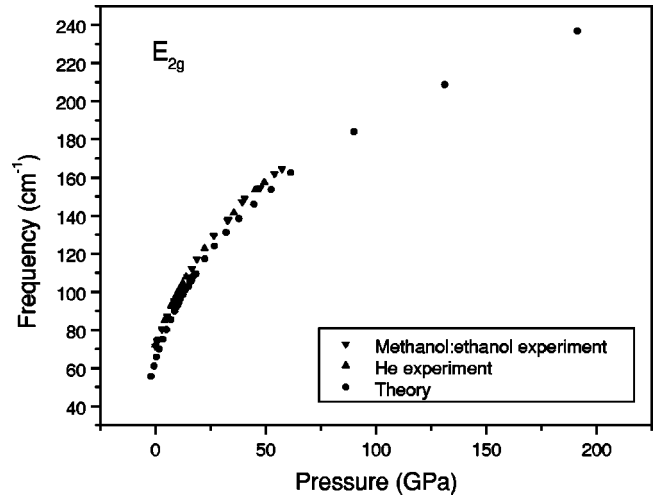


FIG. 2. Zn: E_{2g} mode (theory and experiment).

IV. RESULTS AND DISCUSSION

The hcp lattice has two atoms per primitive unit cell, which are located on sites of symmetry D_{3h} . The six normal modes of zero wave vector belong to the irreducible representations $A_{2u} + B_{1g} + E_{1u} + E_{2g}$. The B_{1g} and E_{2g} modes are the longitudinal and transverse optical modes, respectively. The doubly degenerate E_{2g} mode is Raman active.

Typical Raman spectra of Zn metal at various pressures are shown in Fig. 1. The pressure dependence of the phonon frequencies for the two high-pressure runs are shown in Fig. 2. The E_{2g} mode exhibits a positive pressure shift to maximum pressure. No differences between the two runs were observed. The frequency of the E_{2g} phonon of Zn at ambient conditions in the present study is 71 cm^{-1} and compares favorably with the values obtained from previous ambient pressure Raman scattering^{24–28} and inelastic neutron scattering.^{29–32} The measured frequency-pressure data are well represented by the expression

$$\nu(P)/\nu_0 = [1 - (\delta'_0/\delta_0)P]^{-\delta_0'/\delta_0} \quad (4.1)$$

with ν_0 is the mode frequency at $P=0$ GPa, $\delta_0 = (d \ln \nu/dP)_{P=0}$ the logarithmic pressure coefficient, and δ'_0 the pressure derivative of δ for $P=0$. The parameters are collected in Table I. From the run with He as the pressure-transmitting medium, the pressure dependence of the linewidth is shown in Fig. 3. Initially the half width decreases with increasing pressure, but broadening is observed above 10 GPa to the maximum pressure of 50 GPa.

Figure 2 also shows calculated frequency-pressure data for Zn, at 0 K. Although this figure appears to indicate good agreement between theory and experiment, a closer examination, Fig. 4, reveals marked differences. The calculated frequencies are systematically lower by $\approx 5 \text{ cm}^{-1}$ over the whole pressure range. Since the calculated frequencies refer to 0 K and cooling from room temperature to 4 K results in

TABLE I. Pressure coefficients of the E_{2g} mode of Zn.

	ν_0 (cm^{-1})	δ_0 (GPa^{-1})	δ'_0 (GPa^{-2})
Zn	71.1 ± 0.3	0.05315 ± 0.0015	-0.00728 ± 0.0005

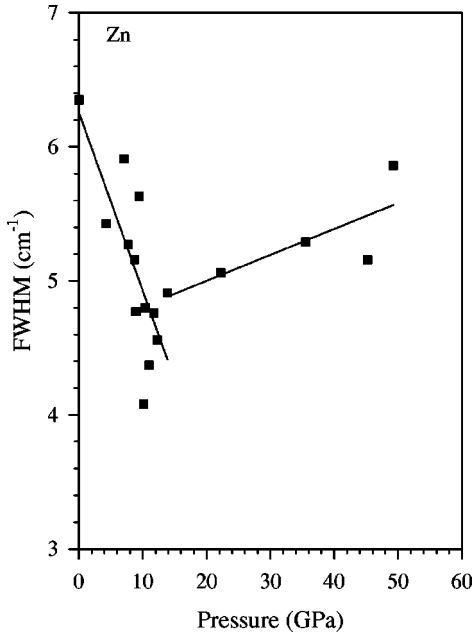


FIG. 3. Pressure dependence of the E_{2g} line width from the run with He as pressure-transmitting medium.

a positive frequency shift of approximately 5 cm^{-1} at ambient pressure,^{22–24} the discrepancy might be slightly higher. According to the calculations ETT's occur for P near 10 GPa, and a very weak anomaly was found ($\approx 0.2\%$) in the c/a ratio near 1.73 (Fig. 5). Nevertheless, no significant signature of this appears in the calculated $\nu(P)$ (Fig. 5). For comparison, we also include, Fig. 6, the calculated frequencies for the B_{1g} mode. The calculated ambient pressure frequency of 152 cm^{-1} is in good agreement with data from inelastic n scattering,^{29–32} which range from $152\text{--}158 \text{ cm}^{-1}$.

The mode Grüneisen parameter

$$\gamma_i = -d \ln \nu_i / d \ln V \quad (4.2)$$

was determined by fitting the $\ln \nu_i(P) - \ln V(P)$ values to a second-order polynomial. The $V(P)$ values were taken from

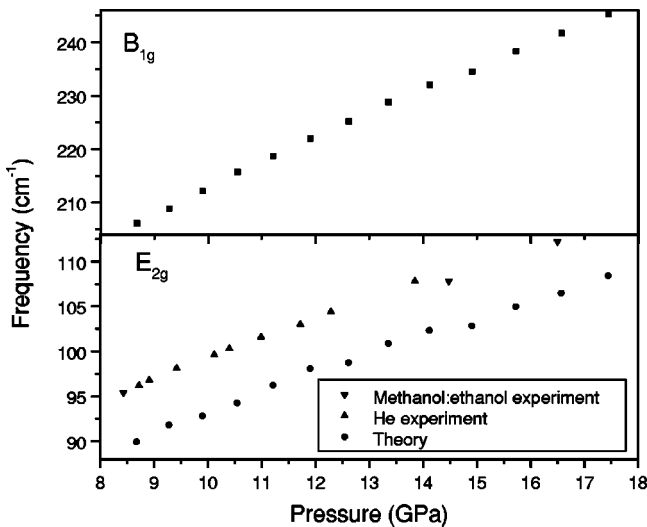


FIG. 4. Zn: E_{2g} and B_{1g} modes.

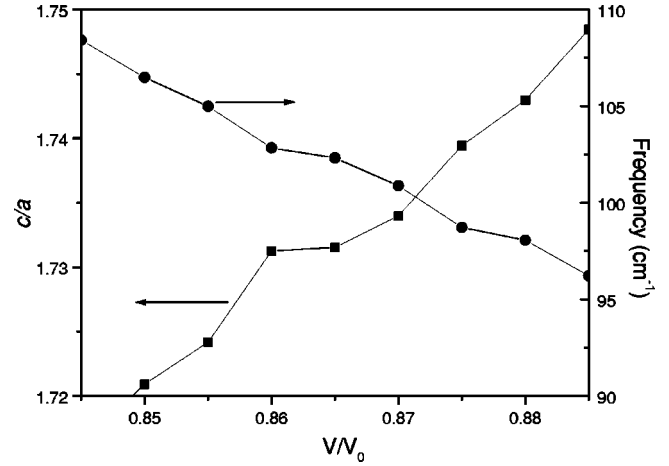


FIG. 5. Zn: E_{2g} mode and c/a (theory).

Takemura's data⁶ using a Birch-Murnaghan equation of state with bulk modulus $B_0 = 65 \text{ GPa}$ and its pressure derivative $B'_0 = 4.6$. In Fig. 7 the E_{2g} mode Grüneisen parameter thus determined is shown as a function of the relative volume together with corresponding data for other hcp metals. In comparison to the other metals, Zn has a relatively high ambient pressure value which shows a relatively rapid decrease under compression. For anisotropic materials it is well known that the values for the mode Grüneisen parameters of different modes show a wide variation. This is due to the fact that the various vibrational modes are controlled by bonds which respond differently with decreasing volume.³⁵ To a first approximation, the frequency ν of the Γ -point TO mode is related to the elastic constant C_{44} by the expression^{36–38}

$$\nu \sim \sqrt{(a^2 C_{44}) / (c \cdot m)}, \quad (4.3)$$

where a and c are the lattice constants and m is the atomic mass. For the mode Grüneisen parameter γ one obtains

$$\gamma = 0.5(B/B_c - 2B/B_a + BC'_{44}/C_{44}), \quad (4.4)$$

where B is the bulk modulus, B_a and B_c are the inverse linear compressibilities of the a and c axes, respectively, and C'_{44} is the pressure derivative of the elastic constant C_{44} . For

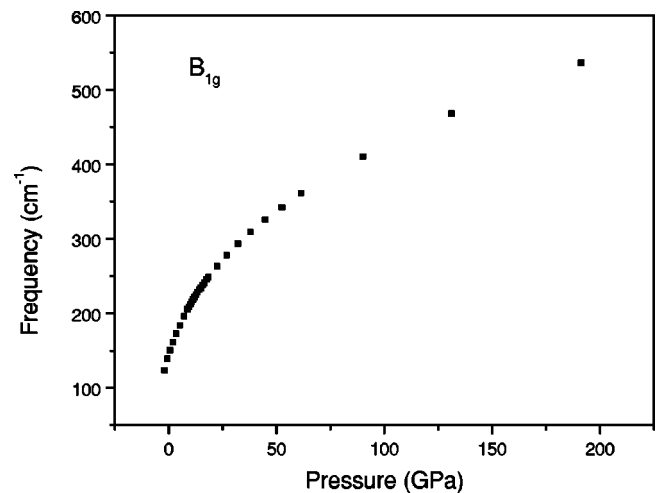


FIG. 6. Zn: B_{1g} mode (theory).

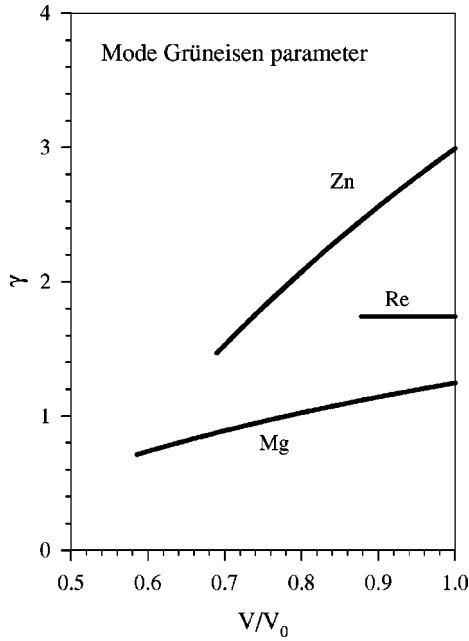


FIG. 7. Experimental E_{2g} mode Grüneisen parameter versus relative volume for Zn, Mg (Ref. 33), and Re (Ref. 34).

hexagonal crystals, the relation between bulk modulus and inverse linear compressibilities is given by

$$B = (B_c B_a) / (2B_c + B_a) \quad (4.5)$$

which reduces to simpler relations for the following limiting cases:

$$\text{Case A: } B_c \ll B_a, \quad B \approx B_c; \quad (4.6)$$

$$\text{Case B: } B_c \approx B_a, \quad B \approx B_c/3 \approx B_a/3; \quad (4.7)$$

$$\text{Case C: } B_c \gg B_a, \quad B \approx B_a/2. \quad (4.8)$$

For Zn at ambient pressure, the inverse linear compressibility B_a is a factor 8–10 larger than B_c which is close to case A. Around 100 GPa both inverse linear compressibilities have approached to the same value indicating that Zn undergoes a gradual anisotropic \rightarrow isotropic transition under pressure as far as the linear compressibilities are concerned, i.e., at 100 GPa case B is more appropriate. Case B also applies for Mg as well as for Re, because for both metals the inverse linear compressibilities of both axes have approximately the same value under compression. The expression for the Grüneisen parameters for Zn at ambient pressure reduces to

$$\gamma = 0.5(1 - 0 + B_c C'_{44}/C_{44}) \quad (4.9)$$

and for Zn around 100 GPa as well as for Mg and Re over their whole compression range, to

$$\gamma = 0.5[1/3 - 2/3 + 1/3(B_c C'_{44}/C_{44})] \quad (4.10)$$

Comparing Eqs. (4.9) and (4.10) it is obvious that all three terms within the parentheses contribute to an extra enhancement of γ for Zn at ambient pressure, which is clearly related to the strong anisotropic compressional behavior of the a and c axis at ambient conditions and under pressure.^{6,10}

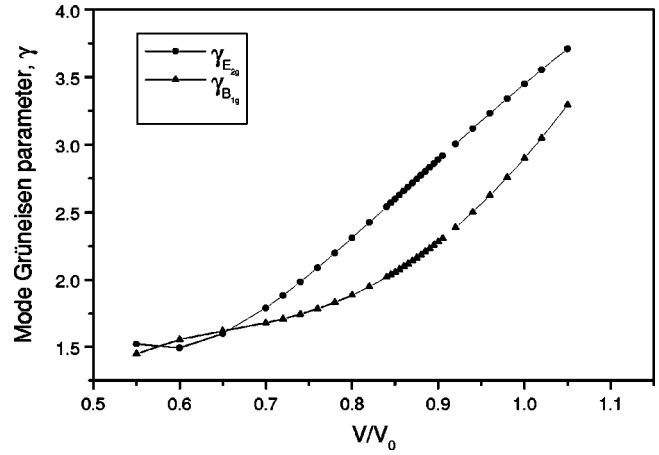


FIG. 8. Calculated B_{1g} and E_{2g} mode Grüneisen parameter versus relative volume for Zn.

One can also note that this enhancement decreases, as the inverse linear compressibilities approach each other, leading to the relatively large decrease of γ observed in Zn under compression. A similar, more pronounced effect is predicted for the Grüneisen parameter of the B_{1g} mode, as shown by a comparison of the theoretically determined volume dependence of the E_{2g} and B_{1g} mode Grüneisen parameters (Fig. 8). B_{1g} is a compressional mode in which successive hexagonal planes are vibrating against each other along the c direction which means that this vibration is controlled by the interactions between the hexagonal layers, which in the case of Zn are much weaker than those within the hexagonal planes. The high ambient pressure value and the strong decrease under compression of the B_{1g} mode Grüneisen parameter can be explained in the same way as in the case of the E_{2g} mode, since to a first approximation, a relation, similar to Eq. (4.4) holds between B_{1g} and the elastic constant C_{33} :^{36–38}

$$\nu \sim \sqrt{(a^2 C_{33}) / (c \cdot m)}. \quad (4.11)$$

The higher ambient pressure Grüneisen parameter of the B_{1g} mode can be traced back to the fact by using Eq. (4.4) that the ratio C'_{33}/C_{33} is about 10% larger than the ratio C'_{44}/C_{44} .^{39,40}

The phonon linewidths originate from the phonon-phonon interaction, the electron-phonon interaction and disorder effects.^{27,28} For zinc it has been shown that at ambient conditions the main contributions to the line width are due to multiphonon anharmonic processes.^{27,28} The observed decrease of the linewidth in the pressure interval 0–10 GPa then may indicate that these anharmonic effects tend to be reduced under pressure at first. The reversal of the pressure dependence of the linewidth occurs at about 10 GPa, where ETT's are thought to occur. One may speculate that these electronic transitions affect the phonon-phonon and/or electron-phonon interactions.

On the other hand, He becomes solid at 11 GPa and the observed increase of the linewidth at higher pressures could also indicate small nonhydrostatic effects due to solidification of He. Furthermore, in Raman studies of polycrystalline samples the restriction to zero wave vector does not hold strictly. Due to the random orientation of the crystallites in

polycrystalline samples the wave vector of the observed Raman phonons covers a maximum range Δk around the Γ point with

$$\Delta k = 2\omega n/c, \quad (4.12)$$

where ω is the frequency of the exciting light, n is the index of refraction of the sample, and c is the speed of light.⁴¹ From this consideration the pressure induced changes in the linewidth might be a consequence of pressure-induced changes in the dispersion around $k=0$ in certain symmetry directions.

V. CONCLUSIONS

The $k=0$ transverse-optical (E_{2g}) phonon mode of Zn metal was observed up to 58 GPa by Raman scattering at room temperature and found to shift to higher frequencies under compression. The frequency increase under pressure is in good agreement, within $\sim 5 \text{ cm}^{-1}$, with recent theoretical calculations. No anomaly in the frequency shift is found

(within 0.2 cm^{-1}) in the pressure range 9–10 GPa, where ETT's are predicted to occur, which suggests that the E_{2g} mode is not well suited for probing these electronic effects, at least at room temperature. In comparison to Mg and Re the mode Grüneisen parameter of Zn has a high value at ambient conditions and shows a strong decrease under compression, which is related to the highly anisotropic compressional behavior of Zn at ambient pressure and the gradual transition to isotropic behavior under compression, respectively. The initial decrease of the E_{2g} linewidth under pressure is followed by a slight increase for pressures above 10 GPa, and might indicate changes in the phonon-phonon and/or electron-phonon interactions that could be related to the electronic transitions.

ACKNOWLEDGMENTS

Support for this project was provided in part by NERC under Contract No. GR9/03546 and by EPSRC under GR/M32597.

-
- ¹R.W. Lynch and H.G. Drickamer, *J. Phys. Chem. Solids* **26**, 69 (1965).
²D.B. McWhan, *J. Appl. Phys.* **36**, 664 (1965).
³O. Schulte, A. Nikolaenko, and W.B. Holzapfel, *High Press. Res.* **6**, 169 (1991).
⁴O. Schulte and W.B. Holzapfel, *Phys. Rev. B* **53**, 569 (1996).
⁵K. Takemura, *Phys. Rev. Lett.* **75**, 1807 (1995).
⁶K. Takemura, *Phys. Rev. B* **56**, 5170 (1997).
⁷K. Takemura, *Phys. Rev. B* **60**, 6171 (1999).
⁸S. Meenahshi, V. Vijayakumar, B. Godwal, and S.K. Sikka, *Phys. Rev. B* **46**, 14 359 (1992).
⁹L. Fast, R. Ahuja, L. Nordström, J. M. Wills, B. Johansson, and O. Eriksson, *Phys. Rev. Lett.* **79**, 2301 (1997).
¹⁰D.L. Novikov, A.J. Freeman, N.E. Christensen, A. Svane, and C.O. Rodriguez, *Phys. Rev. B* **56**, 7206 (1997).
¹¹D.L. Novikov, M.I. Katsnelson, A.V. Trefilov, A.J. Freeman, N.E. Christensen, A. Svane, and C.O. Rodriguez, *Phys. Rev. B* **59**, 4557 (1999).
¹²W. Potzel, M. Steiner, H. Karzel, W. Schiessl, M. Köfferlein, G.M. Kalvius, and P. Blaha, *Phys. Rev. Lett.* **74**, 1139 (1995).
¹³M. Steiner, W. Potzel, H. Karzel, W. Schiessl, M. Köfferlein, G.M. Kalvius, and P. Blaha, *J. Phys.: Condens. Matter* **8**, 3581 (1996).
¹⁴J.G. Morgan, R.B. Von Dreele, P. Wochner, and S.M. Shapiro, *Phys. Rev. B* **54**, 812 (1996).
¹⁵S. Klotz, M. Braden, and J.M. Besson, *Phys. Rev. Lett.* **81**, 1239 (1998).
¹⁶A.P. Jephcoat, H.K. Mao, and P. Bell, *Hydrothermal Experimental Techniques*, edited by G.C. Ulmer and H.L. Barnes (Wiley Interscience, New York, 1987), p. 469.
¹⁷R.A. Forman, G.J. Piermarini, J.D. Barnett, and S. Block, *Science* **176**, 284 (1972).
¹⁸H.K. Mao, P.M. Bell, J.W. Shaner, and D.J. Steinberg, *J. Appl. Phys.* **49**, 3276 (1978).
¹⁹O.K. Andersen, *Phys. Rev. B* **12**, 3060 (1975).
²⁰M. Methfessel, *Phys. Rev. B* **38**, 1537 (1988).
²¹M. Methfessel and M. van Schilfhaarde (unpublished).
²²J.P. Perdew, K. Burke, and M. Ernzerhof, *Phys. Rev. Lett.* **77**, 3865 (1996).
²³N.E. Christensen, in *High Pressure in Semiconductor Physics*, edited by T. Suski and W. Paul, Vol. 54 of *Semiconductors and Semimetals*, edited by R.K. Willardson and E.R. Weber (Academic Press, New York, 1998), p. 49.
²⁴D.W. Feldman, J.H. Parker, Jr., and M. Ashkin, *Phys. Rev. Lett.* **21**, 607 (1968).
²⁵J.H. Parker, Jr., D.W. Feldman, and M. Ashkin, in *Light Scattering Spectra of Solids*, edited by G.B. Wright (Springer-Verlag, New York, 1969), p. 389.
²⁶W.B. Grant, H. Schulz, S. Hüfner, and J. Pelzl, *Phys. Status Solidi B* **60**, 331 (1973).
²⁷H. Schulz and S. Hüfner, *Solid State Commun.* **20**, 827 (1976).
²⁸V.V. Baptizmanskii, I.I. Novak, and A.F. Naidenov, *Fiz. Tverd. Tela (Leningrad)* **21**, 2584 (1979) [*Sov. Phys. Solid State* **21**, 1488 (1979)].
²⁹G. Borgonovoi, C. Caglioti, and J.J. Antal, *Phys. Rev.* **132**, 683 (1963).
³⁰P.K. Iyengar, Y.H. Gameel, K.R. Rao, and G. Venkataraman (unpublished).
³¹D.L. McDonald, M.M. Elombe, and A.W. Pryor, *J. Phys. C* **2**, 1857 (1969).
³²L. Almquist and R. Stedman, *J. Phys. F* **1**, 785 (1971).
³³H. Olijnyk, *J. Phys.: Condens. Matter* **11**, 6589 (1999).
³⁴H. Olijnyk and A.P. Jephcoat (unpublished).
³⁵W.F. Sherman, *J. Phys. C* **13**, 4601 (1980).
³⁶E.A. Metzbowyer, *Phys. Status Solidi* **25**, 403 (1968).
³⁷M.P. Verma and J.C. Upadhyaya, *Solid State Commun.* **13**, 779 (1973).
³⁸J.C. Upadhyaya, D.K. Sharma, D. Prakash, and S.C. Upadhyaya, *Can. J. Phys.* **72**, 61 (1994).
³⁹G.A. Alers and J.R. Neighbours, *J. Phys. Chem. Solids* **7**, 58 (1958).
⁴⁰K.D. Swartz and C. Elbaum, *Phys. Rev. B* **1**, 1512 (1970).
⁴¹N.W. Ashcroft and N.D. Mermin, *Solid State Physics* (Saunders College, Philadelphia, 1976), p. 482.